Soil Aquifer Treatment System Design Equation for Organic Micropollutant Removal

Ahmed M. Abdel Sattar, Hossein Bonakdari, Abdelazim Negm, Bahram Gharabaghi, and Mohamed Elhakeem

Abstract Rapid population growth and mass migration from rural to urban centers have contributed to a new era of water sacristy, and a significant drop in per capita freshwater availability, resulting in the reuse of wastewater emerging as a viable alternative. The reuse of wastewater after treatment using the soil aquifer treatment (SAT) has recently gained popularity due to low operating/maintenance cost of the method. However, the presence of organic micropollutants (OMPs) may present a health risk if the SAT is not adequately designed to ensure required attenuation of the OMPs. An important aspect of the design of the SAT system is the large degree of natural variability in the OMP concentrations/loads in the wastewater and the uncertainty associated with the current methods for calculation of the removal efficiency of

A.M. Abdel Sattar (✉)
Department of Irrigation and Hydraulics, Faculty of Engineering, Cairo University, Giza, Egypt

German University in Cairo, New Cairo, Egypt
e-mail: ahmoudy77@yahoo.com

H. Bonakdari
Department of Civil Engineering, Razi University, Kermanshah, Iran

A. Negm
Department of Water and Water Structures Engineering, Faculty of Engineering, Zagazig University, Zagazig, Egypt
e-mail: amnegm@zu.edu.eg

B. Gharabaghi
School of Engineering, University of Guelph, Guelph, ON, Canada

M. Elhakeem
University of Tennessee, Knoxville, TN, USA

Abu Dhabi University, Abu Dhabi, United Arab Emirates
e-mail: mohamed.elhakeem@adu.ac.ae

the SAT for the OMPs. This study presents a novel model for more accurate prediction of the removal efficiency of the SAT system for the OMPs and the fate of the OMPs trapped within the vadose zone. A large data set is compiled covering a broad range of aquifer conditions, and the SAT system parameters, including hydraulic loading rate and dry/wet ratio. This study suggests that removal of OMPs in SAT systems is most affected by biodegradation rate and soil saturated hydraulic conductivity, in addition to dry to wet ratio. This conclusion is reached by the application of the developed prediction model using data sets from the case study SAT systems in Egypt.

Contents

1   Introduction

SAT system is considered attractive unconventional water resources for Egypt, which is suffering water sacristy. The usage of SAT can provide treatment for the wastewater and recharge in groundwater aquifers. While guidelines are available for the use of SAT system in Egypt for removal of nitrogen and organic matter, no guidelines are available for the SAT removal potential of organic micropollutants. This chapter discusses this issue and provides a prediction model for the OMP removal in SAT systems and is based on the author's work on soil aquifer treatment system and analysis models [1–21].
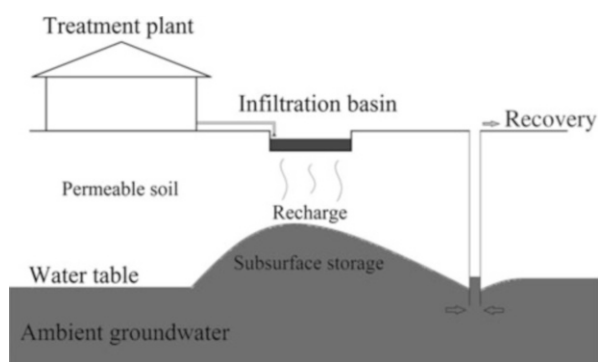
2   Soil Aquifer Treatment System

The increasing development of urbanization and population growth has been caused by water resource pollution control and proper recharge of soil aquifer. There is the possibility of organic micropollutants (OMPs) into the aquifer during groundwater aquifer recharge. Organic micropollutants consist of toxic minerals of endocrine disruptors, pharmaceutically active compounds, and personal care product. The environmental and health risks are increased by entering of the organic micropollutants into an aquifer soil. Therefore, the control and elimination of organic micropollutants from soil aquifer treatment system are of paramount importance to protect the aquifer from pollution. Because of the importance of control and removal of organic micropollutants from water resources, many studies have been conducted to remove these compounds. Drillia et al. [22] in an experimental study removed six different pharmaceutical compounds from various soils for municipal wastewater. Xu et al. [23] using the degradation and adsorption removed the personal care products and pharmaceuticals in agricultural soils in an experimental study. Maeng et al. [24] examined the OMP removal during bank penetration and feeding and recovery of aquifers. Time and place of transfer were provided to remove the active pharmaceutical ingredients. Yu et al. [25] studied three different soil types to remove the five types of pharmaceuticals and personal care products (PPCPs). Also, they studied the seasonal changes of organic micropollutant compounds in sewage treatment plant (STP). Personal care products and endocrine-disrupting were removed from the California wastewater.

Soil aquifer treatment (SAT) is a perfect option to artificial recharge of the groundwater aquifer. On the other hand, there is likely the penetration of the organic micropollutants (OMPs) into the soil aquifer during soil aquifer treatment as well. Hence, OMP removal in SAT system is of considerable importance. In Fig. 1, a schematic plan of soil aquifer treatment system at a sewage treatment station has been shown.

Lin et al. [26] eliminated the heavy metals for soil aquifer treatment in a wastewater treatment plant. Also, Fox et al. [27] in an experimental study analyzed the organic carbon content in the soil aquifer treatment for the five different types of

Fig. 1 Schematic plan of soil aquifer treatment system at a sewage treatment plant

soil. Amy and Drewes [28] investigated the removal/transformation mechanism of organic matter from wastewater stream through the soil aquifer treatment for wastewater treatment plant. Then, Sharma et al. [29] analyzed the removal of organic materials in wastewater during soil aquifer treatment system. Their results showed that the redox conditions, input flow rate, and residence time are sufficient for the removal of organic waste. Xu et al. [23] studied the characteristics and behavior of dissolved organic matter on the soil aquifer treatment. It was also showed that during soil aquifer treatment, 70% of the organic material is removed. Also, Caballero [30] studied the SAT system as a pretreatment process to remove organic micropollutant compounds from the wastewater stream. Sharma et al. [29] analyzed the effects of horizontal roughing filtration, coagulation, and sedimentation during pretreatment operations on the mechanism of soil aquifer treatment. It was showed that sedimentation and coagulation lead to less head loss and reduce the clogging effects. Abel et al. [31] examined the effects of temperature and redox conditions on the reduction of organic matter of wastewater on the soil columns and SAT systems. Abel et al. [31] studied the organic matter reduction, pharmaceutical compounds, and nitrogen in the soil aquifer treatment process in a laboratory model. Onesios-Barry et al. [32] conducted an experimental study of the SAT system in the removal of pharmaceuticals and personal care products (PPCPs) for different concentrations in wastewater treatment plants. Suzuki et al. [33] studied the mechanism of the organic matter removal and disinfection by-product formation potential in the higher layer of the soil aquifer treatment system in an experimental study.

3 Simulations of SAT Organic Micropollutant Removal

3.1 Model Setup

To capture the change in characteristics of OMPs during infiltration in the vadose zone, Sattar [13] chose a 2D vertical section in the soil beneath the SAT pond. Study domain dimensions were taken (10 m × 30 m). The upper boundary was selected to be a variable flux boundary of width 5 m, to simulate the intermittent water infiltration from a spreading basin, and lies in the center of the domain width. The lower boundary is chosen as free drainage to allow flow passage below the study domain. The OMP attenuation was simulated throughout 90 days from the day of application of wastewater in the ponds. This time was considered sufficient for OMP plume to infiltrate through soil layers and gets attenuated.

3.2 Attenuation of OMPs in SAT System

Using the average values of the SAT system parameters presented in Sattar [11], HYDRUS simulations were carried to model the fate of OMPs in SAT system under
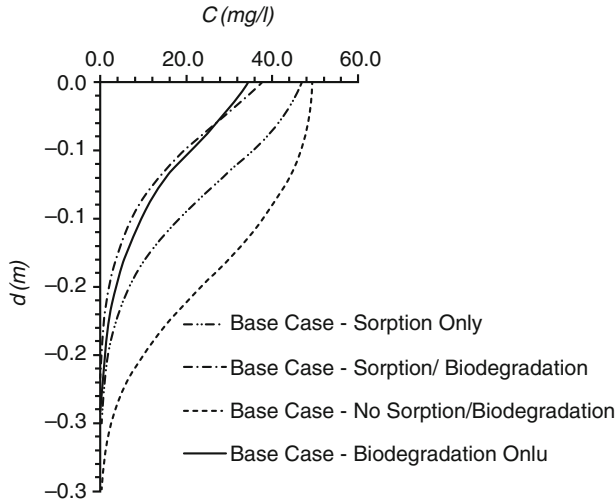
Fig. 2 Variation of OMPs along depth

effects of sorption and biodegradation, both individually and combined. Figure 2 shows the variation of OMP concentration along the depth of vadose zone captured along the vertical centerline of the study domain. It was clear that the biodegradation process was more efficient in reducing the contaminant concentration than the sorption process although the plume sizes for both simulations were almost the same after 90 days. Moreover, it was noted that the OMP concentration at the topsoil layer was higher, in case of considering both sorption and biodegradation than in case of considering biodegradation only. The reason for this was attributed to the effect of sorption which distributes the contaminant mass between the sorbed phase and the liquid phase soon after the contaminant injection which explains the lower concentration after day 86. On the other side, biodegradation process is only active for the contaminant mass existing in the liquid phase which means that the mass that is sorbed onto the soil is not available for biodegradation. This leads to higher biodegradation rates in the case of biodegradation only than the case of combined sorption and biodegradation.

4 Extreme Learning Machine

Various studies have been conducted concerning to the use of artificial intelligence in performance evaluation of SAT system. Recently, Sattar [11] predicted the organic micropollutant removal during soil aquifer treatment system by gene expression programming model.

One of the most popular technique in data mining field is feedforward neural network (FFNN) which is trained by a gradient-descent algorithm such as back-

propagation (BP). The disadvantages of FFNN-BP which lead to the low performance of this technique are imprecise learning rate and slow rate of convergence and presence of local minima. Therefore, Huang et al. [34] introduced a new algorithm for FFNN training based on single hidden layer feedforward neural networks (SLFNs), namely, extreme learning machine (ELM). The ELM required adjusting only activation function type and a number of hidden layers, while there are several user-defined parameters such as adjustment of hidden layer biases during execution of the algorithm and input weights. ELM compared to other learning algorithms such as BP in the learning process perform very fast and present appropriate performance in extended processing generation function. In this study, the removal mechanism of organic micropollutants (OMPs) in soil aquifer treatment (SAT) using extreme learning machine (ELM) method is modeled.

4.1 Architecture of ELM

Huang et al. [34] presented a new algorithm in terms of extreme learning machine learning to train the single-layer feedforward neural network (SLFFNN) as it does not require iterative tuning and has the ability to achieve global minima. The use of ELM in training the SLFFNN leads to a significant reduction in training time compared to the algorithms based on gradient-descent. Also, the use of active ELM as training algorithm does not require additional parameters such as stopping criterion and learning rate. Experimental observations by Huang et al. [34] showed that the ELM has an excellent ability in universal approximation and useful generalization. In an SLFFNN with random hidden nodes, at first, the input data set and real actual output of the model $[(X), (Y)]$ are determined. Subsequently, the number of hidden nodes $[K]$ and the type of activation function $[g(\cdot)]$ are determined. Then, its weight and bias values are presented in random order $[(W), (b)]$. Then, the hidden layers' matrix $[H]$ is determined, and then the weight of output as analytic is calculated $[\beta]$. Input variables can be defined as the following matrix:

$$X = \begin{bmatrix} X_{11} & \cdots & X_{1j} \\ \vdots & \cdots & \vdots \\ X_{n1} & \cdots & X_{nj} \end{bmatrix}_{n \times j} \tag{1}$$

where n and j are the numbers of samples and variables, respectively. Also, the actual output is defined as follows:

$$Y = \begin{bmatrix} Y_1 & \cdots & Y_n \end{bmatrix}^T \tag{2}$$

In the following, a positive integer value for hidden nodes (K) and a differentiable function for $g(\cdot)$ should be defined. Thus, an input weight matrix W is created randomly to make the connection between the input and hidden nodes:

$$W = \begin{bmatrix} W_{11} & \cdots & W_{1k} \\ \vdots & \cdots & \vdots \\ W_{j1} & \cdots & W_{jk} \end{bmatrix}_{j \times k} \tag{3}$$

Hidden layer matrix H by multiplying the input matrix X in the weight matrix W is calculated as follows:

$$H = XW \tag{4}$$

Hidden layer active matrix H with the function $g(\cdot)$ leads to the hidden layer output matrix:

$$H = g(H) \tag{5}$$

Output matrix of the hidden layer, H_{out}, and an input vector $\hat{Y}$ by output layer weight β are connected. ELM network output is calculated as follows:

$$\hat{Y} = H_{\text{out}}\beta \tag{6}$$

and

$$\left\| H_{\text{out}}\widehat{\beta} - Y \right\| = \min_{\beta} \| H_{\text{out}}\beta - Y \| \tag{7}$$

The minimum norm to solve the least squares is calculated as follows:

$$\beta = H_{\text{out}}^{+}Y \tag{8}$$

where H_{out}^{+} calculated as follows is the Moore-Penrose generalized inverse of H_{out}:

$$H_{\text{out}}^{+} = \left(H^{T}H\right)^{-1}H^{T} \tag{9}$$

4.2   Performance Evaluation Criteria

In this study, to investigate the accuracy of numerical models, statistical indices root-mean-square error (RMSE), mean absolute percentage error (MARE), correlation coefficient (R), BIAS, scatter index (SI), and ρ are used as follows:

$$\text{RMSE} = \sqrt{\frac{1}{n'} \sum_{i=1}^{n'} \left(T_{(\text{Predicted})_i} - T_{(\text{Observed})_i}\right)^2} \tag{10}$$

$$\text{MARE} = \frac{1}{n'} \sum_{i=1}^{n'} \left(\frac{\left| T_{(\text{Predicted})_i} - T_{(\text{Observed})_i} \right|}{T_{(\text{Observed})_i}} \right) \tag{11}$$

$$\text{BIAS} = \frac{1}{n'} \sum_{i=1}^{n'} \left(T_{(\text{Predicted})_i} - T_{(\text{Observed})_i} \right) \tag{12}$$

$$R = \frac{\sum_{i=1}^{n'} \left(T_{(\text{Observed})i} - \bar{T}_{(\text{Observed})} \right) \left(T_{(\text{Predicted})i} - \bar{T}_{(\text{Predicted})} \right)}{\sqrt{\sum_{i=1}^{n'} \left(T_{(\text{Observed})i} - T_{(\text{Observed})} \right)^2 \sum_{i=1}^{n'} \left(T_{(\text{Predicted})i} - \bar{T}_{(\text{Predicted})} \right)^2}} \tag{13}$$

$$\text{SI} = \frac{\text{RMSE}}{\bar{T}_{(\text{Observed})}} \tag{14}$$

$$\rho = \frac{\text{SI}}{1 + R} \tag{15}$$

where $T_{(\text{Observed})i}$ is the observed values, $T_{(\text{Predicted})i}$ the predicted values by the numerical model, $\bar{T}_{(\text{Observed})i}$ the mean of observed values, and n' the number of observed data.

5 ELM Prediction of SAT Organic Micropollutant Removal

Table 1 shows the parameters controlling the operation of a SAT system and the removal of OMPs, while Table 2 illustrates the ranking of parameters according to their contribution on the removal of OMPs in a SAT system [35]. It is observed that three parameters had the highest ranking: first-order biodegradation rate, saturated hydraulic conductivity, and dry to wet ratio. These high influential parameters have been chosen as predictors for developing prediction models in Sattar [11] and in this study. Using the 50,000 data sets simulated by Sattar [11], 25,000 (50%) were used to develop the models, 12,500 (25%) were used to test the models, and 12,500 (25%) were used to validate the developed models.

To develop an OMP attenuation prediction model, the OMP plume mass, normalized mass ratio, and zero concentration depth are addressed. The mass stored in the contaminant plume can be calculated as:

$$\text{Plume Mass} = V \times \sum_{i=1}^{N} C_i \cdot \theta_i \tag{16}$$

where N = the total number of 2D FE mesh nodes in the study domain, i = the index of the node number, C_i = contaminant concentration at node i, θ_i = unsaturated moisture content at node i, and V = soil volume of each node.

Table 1 Parameters controlling the fate and transport of OMPs in SAT system [11]

Parameter classes	Parameter	Min.	Max.	Avg.
Soil hydraulic	Residual water content, θ_r (cm^3/cm^3)	0.024	0.066	0.045
	Saturated water content, θ_s (cm^3/cm^3)	0.364	0.448	0.406
	Saturated hydraulic conductivity, K_s (cm/day)	20	800	410
	Van Genuchten parameter, α (1/cm)	0.0059	0.0514	0.0287
	Van Genuchten parameter, n	1.34	3.54	2.44
OMP transport and fate	Freundlich coefficient, K_f ((µg kg^{-1}/µg l^{-1}) η)	0.1	500	250.1
	Freundlich exponent, n	0.40	1.6	1
	First-order biodegradation rate, μ_1 (day^{-1})	0.01	0.85	0.43
	Soil bulk density, ρ_b (gm/cm^3)	1.35	1.85	1.6
	Longitudinal dispersivity, α_L (cm)	30	300	165
	Ratio long./trans. dispersivity, α_T/α_L	0.05	0.1667	0.1084
	Molecular diffusion, D_d (cm^2/day)	0.9	1.7	1.3
Operation	HLR/K_s	0.05	0.12	0.085
	HLR (cm/day)	1	95	48
	Initial concentration, C_{in} (µg/l)	0.01	100	50.0
	Dry to wet ratio, DWR	1	7	4

Table 2 Ranking parameters controlling the fate and transport of OMPs in SAT system according to their contribution in system output uncertainty [11]

Parameters classes	Parameter	% importance
0% concentration depth (depth under SAT pond where OMPs are completely attenuated)	First-order biodegradation rate, μ_1 (day^{-1})	48.80
	Saturated hydraulic conductivity, K_s (cm/day)	36.50
	Dry to wet ratio, DWR	6.90
	HLR/K_s	4.30
Plume mass (OMP mass stored in contaminant plume)	First-order biodegradation rate, μ_1 (day^{-1})	66.39
	Initial concentration C_{in} (µg/l)	13.33
	Saturated hydraulic conductivity, K_s (cm/day)	12.05
	Dry to wet ratio, DWR	5.25
Plume normalized mass ratio (ratio of plume mass and cumulative total injected mass)	First-order biodegradation rate, μ_1 (day^{-1})	94.57
	Dry to wet ratio, DWR	5.25

To assess the SAT system OMP removal efficiency, the normalized plume mass has to be calculated, where a system with high removal efficiency would yield smaller fractions of the normalized mass. The normalized plume mass can be calculated as the ratio between the plume mass to the cumulative total injected mass, with time.

Parameter	Maximum	Minimum	Average
Ks (cm/day)	800	20	410
μ_1 (day^{-1})	0.85	0.01	0.43
HLR (cm/day)	95	1	48
C_0 (µg/l)	100	0.01	50.0
DWR	7	1	4

Table 3 The quantities needed for modeling the OMP removal by ELM model

To estimate the parameters of plume mass, normalized mass ratio and concentration depth of 0% of the five parameters are presented in Table 3, as ELM model inputs are used. Therefore, a total of 15 different models of ELM are introduced. It should be noted that the Monte Carlo simulation (MCS) to determine the uncertainty of plume mass, normalized mass ratio, and concentration depth of 0% with 1,000 realizations to generate random inputs of ELM models are used. Sattar [11] stated that the plume mass for organic micropollutants in the soil, 90 days after the SAT operation, is calculated as follows:

$$\text{Plume mass} = 6.14 K_s^{1.1} C_0 \mu_1^{-1} \text{DWR}^{1/2} \tag{17}$$

Here, K_s is saturated hydraulic conductivity, C_0 the amount of concentration, μ_1 the rate of first-order biodegradation, and DWR the intermittent application of wastewater in the soil aquifer treatment system. Also, to calculate the normalized mass ratio, the following equation was used:

$$\text{Mass ratio} = 0.0055_0 \mu_1^{-1} \text{DWR}^{1/5} \tag{18}$$

The minimum depth under a SAT system required to remove more than 98% contamination to the depth of 0% concentration is defined as follows:

$$Y_{\text{zero}} = 0.17 e^{\text{DWR}^{0.5} K_s^{-1}} \mu_1^{-1/2} \text{HLR}^{1/2} \text{DWR}^{-3/8} K_s^{1/4} \tag{19}$$

where HLR is the hydraulic loading rate.

5.1 Plume Mass

Plume mass parameter is calculated by Eq. (16). The results of ELM models 1–5 for this parameter with GEP model provided by Sattar [11] were compared. In Table 4, different statistical indices for ELM models 1–5 and Sattar [11] model in the prediction of plume mass parameter are arranged. Also, scattering plots of the models for plume mass are depicted in Fig. 3. The highest correlation coefficient value for ELM 2 and ELM 5 models is calculated. The lowest of R value for ELM 4 equal to 0.964 is computed. The SI and ρ values for ELM 4 have been predicted, 0.811 and 0.413, respectively. ELM 5 among all ELM models has the highest correlation coefficient value and the least amount of errors. For this model, the

Table 4 Statistical indices of ELM models 1–5 and [11] to predict the plume mass parameter

	Plume mass					
	RMSE	MARE	R	BIAS	SI	ρ
[11]	731,788.8	38.274	0.933	6,603.806	1.073	0.555
ELM 1	527,939.2	6.164	0.968	132,269.1	0.774	0.393
ELM 2	514,951.5	5.625	0.970	116,093.1	0.755	0.383
ELM 3	527,269.9	5.634	0.968	118,727.1	0.773	0.393
ELM 4	553,288	5.272	0.964	−120,723	0.811	0.413
ELM 5	508,715.7	5.473	0.970	−113,364	0.746	0.379

BIAS value is predicted which is − 113,364. However, the MARE and the correlation coefficient values for the Sattar [11] model have been calculated, 38.274 and 0.933, respectively.

5.2 Mass Ratio

In the following, the results of ELM models 1–5 to predict the mass ratio parameter are evaluated. In Table 5, statistical index values to predict the mass ratio by ELM models [11] are shown. Also, scatter plots for the model presented in Fig. 4 are visible. Based on the results of ELM, the highest RMSE value has been predicted for ELM 1 (RMSE = 0.019). For this model, the R statistical index is calculated to equal to 0.974, while ELM 3 has the highest amount of correlation ($R = 0.977$) and the lowest MARE value(MARE = 1.661). For ELM 3, BIAS and ρ parameter are calculated, 0.0036 and 0.239, respectively. In contrast, GEP model introduced by Sattar [11] has less correlation ($R = 0.823$). Hence, RMSE and MARE values for the model [11] have been calculated, 0.521 and 341.867, respectively. Therefore, ELM models to predict the mass ratio parameter have an acceptable accuracy.

5.3 Zero Concentration Depth

Also, the accuracy of ELM models 1–5 in the modeling of Y_{zero} parameter is examined (see Fig. 5). In Table 6, statistical indices calculated for ELM models and GEP model proposed by Sattar [11] are shown. ELM 1 between the ELM models has the least accuracy. For this model, RMSE and ρ values are calculated, 1.479 and 0.145, respectively. However, the value of correlation coefficient for ELM 1 is estimated, 0.959. Also, ELM 5 predicts the Y_{zero} parameter more accurately compared to other ELM models. The parameters MARE, BIAS, and ρ values for this model are predicted, 0.237, 0.00106, and 0.141, respectively. However, the accuracy of the model [11] to predict Y_{zero} parameter is less than ELM models. In other words, the correlation coefficient value for the model is
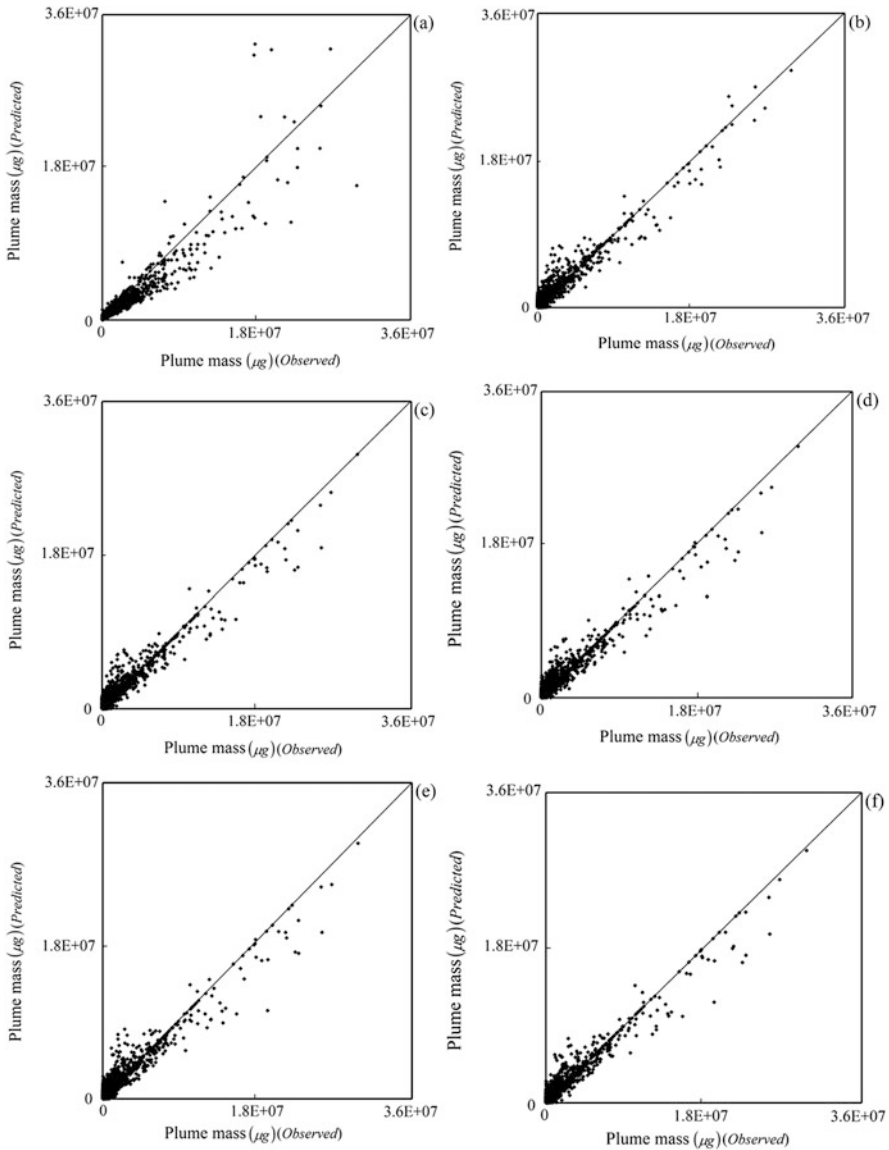
Fig. 3 Scatter plot for prediction of plume mass parameter (**a**) Sattar [11–13] (**b**) ELM 1 (**c**) ELM 2 (**d**) ELM 3 (**e**) ELM 4 (**f**) ELM 5

0.944 [11]. Therefore, based on the analysis of simulation results, ELM model estimates parameters plume mass, mass ratio, and Y_{zero} with reasonable accuracy.

To analyze the results of ELM, the parameter discrepancy ratio (DR) as the ratio of modeled values to measured values is introduced ($DR = T_{(Predicted)}/T_{(Observed)}$) [11]. The proximity of discrepancy ratio to 1 represents the proximity of predicted

Table 5 Statistical indices of ELM models 1–5 and [11] to predict mass ratio parameter

	Mass ratio					
	RMSE	MARE	R	BIAS	SI	ρ
[11]	0.521	341.867	0.823	0.213	13.821	78.084
ELM 1	0.019	5.848	0.974	0.0040	0.494	0.250
ELM 2	0.018	1.979	0.976	0.0039	0.488	0.247
ELM 3	0.018	1.661	0.977	0.0036	0.472	0.239
ELM 4	0.018	1.714	0.976	0.0038	0.480	0.243
ELM 5	0.018	1.807	0.977	0.0037	0.471	0.238

values to measured results. In Table 7, the values DR_{max}, DR_{min}, and DR_{ave} are the maximum, minimum, and mean discrepancy ratio. For plume mass parameter, the lowest DR_{ave} for ELM 4 is calculated, while the average of discrepancy ratio for the model has been computed, 39.175 [11]. For ELM 3, the mass ratio parameter has the lowest DR_{ave} value ($DR_{ave} = 2.508$). The DR_{max} and DR_{min} values for this table model have been estimated, 335.291 and 0.0004, respectively. As can be seen, the DR_{ave} for the proposed GEP model [11] has been obtained, 342.861. The lowest DR_{ave} value to ELM models in prediction of Y_{zero} parameter for ELM 5 is obtained ($DR_{ave} = 1.060$). The DR_{max} and DR_{min} values for the model ELM 5 have been calculated, 65.876 and 0.022, respectively. For model DR_{max}, DR_{min} and DR_{ave} values are obtained, 109.803, 0.545 and 1.250, respectively [11]. Based on the analysis results of discrepancy ratio parameter, results predicted by the model's ELM compared with GEP model introduced by Sattar [11] are closer to the measured values.

6 SAT Site Selection in Egypt

SAT systems would be an attractive unconventional water resource in Egypt, which is true, especially in rural communities. Egyptian researchers are keeping this in mind. Recently, RIGW [36] published recommended characteristics of groundwater aquifer for a successful and efficient SAT operation and removal of organic matter. These included an infiltration rate of more than 0.25 m/day, minimum depth to groundwater of 5 m, high values of porosity, and saturated zone transmissivity, and most importantly, the aquifer should not be flowing into the Nile River. Recently, El Arabi et al. [37] have provided guidelines for the selection of potential SAT sites in Egypt. The primary target for these guidelines was to ensure adequate removal of nitrogen and biochemical oxygen demand (BOD) from treated wastewater. However, the OMP removal criterion has not been considered in these guidelines despite the ecological and health risks imposed by their presence in Egyptian soils and native groundwater. Figure 6 shows the potential locations for construction of SAT systems in Egypt [38]. It was found that the best sites existed on the Western fringes of the Nile delta, W1 to W6, as shown in Fig. 6. SAT
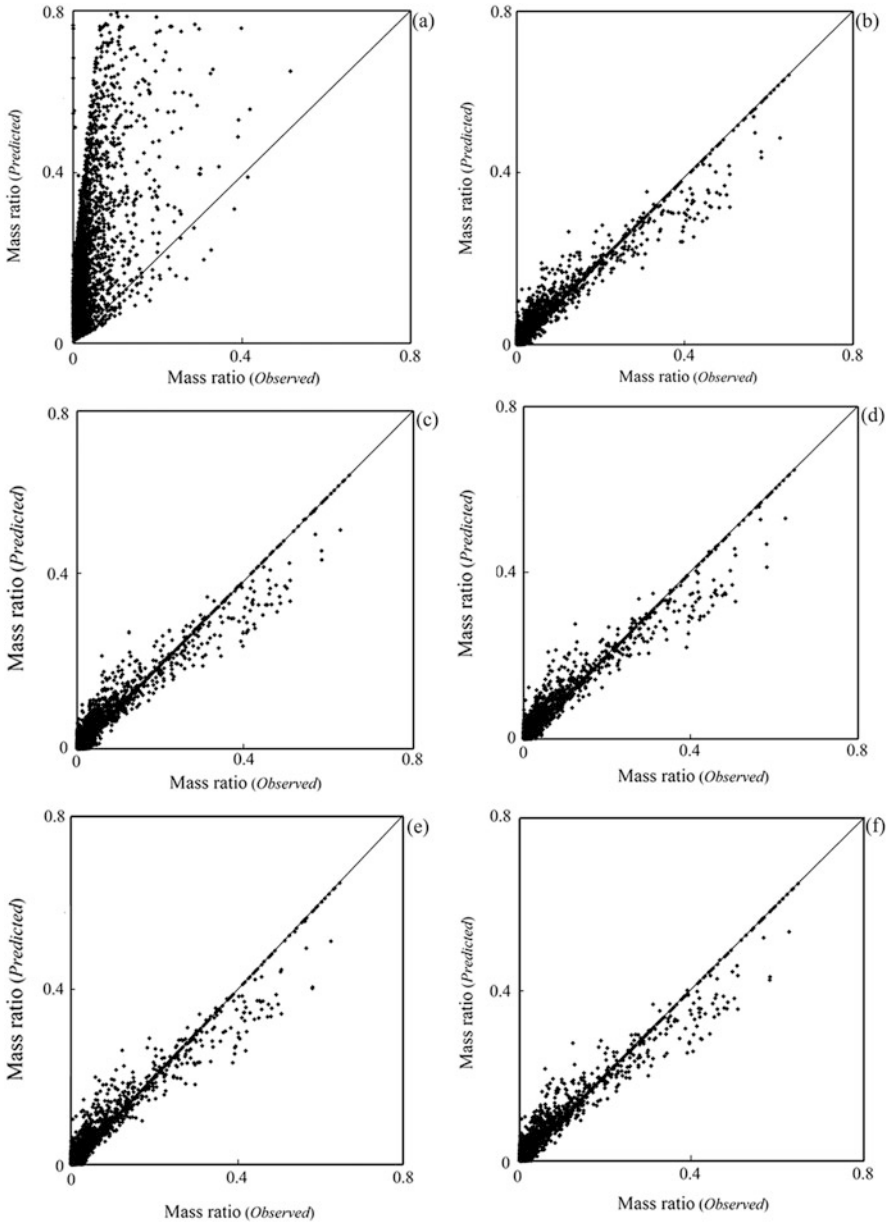
Fig. 4 Scatter plots for prediction of mass ratio parameter (**a**) Sattar [11–13] (**b**) ELM 1 (**c**) ELM 2 (**d**) ELM 3 (**e**) ELM 4 (**f**) ELM 5
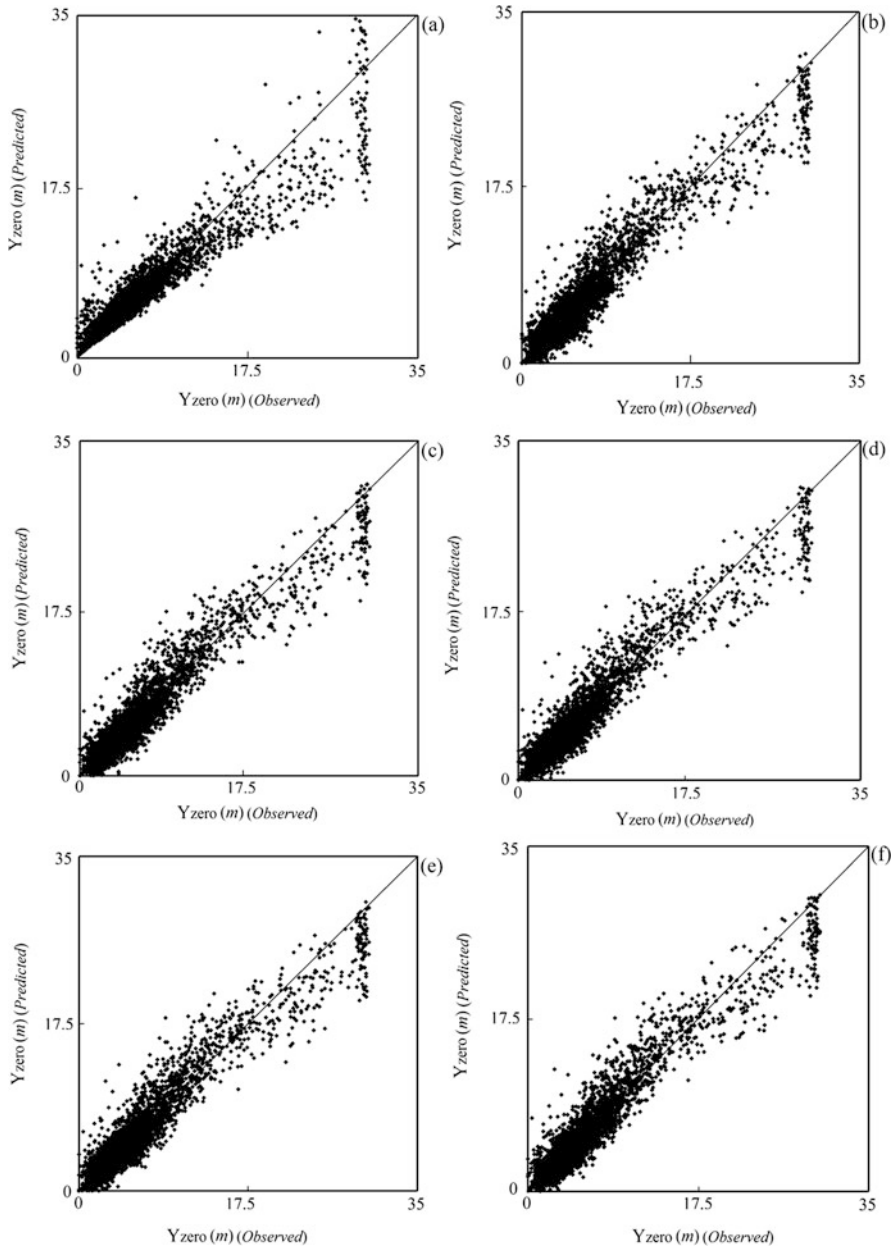
Fig. 5 Scatter plot for prediction of Y_{zero} parameter (**a**) Sattar [11–13] (**b**) ELM 1 (**c**) ELM 2 (**d**) ELM 3 (**e**) ELM 4 (**f**) ELM 5

Table 6 Statistical indices of ELM models 1–5 and [11] to predict the parameter Y_{zero}

	Y_{zero}					
	RMSE	MARE	R	BIAS	SI	ρ
[11]	1.748	0.325	0.944	0.16620	0.335	0.172
ELM 1	1.479	0.252	0.959	0.00115	0.283	0.145
ELM 2	1.457	0.243	0.961	0.00109	0.279	0.142
ELM 3	1.454	0.250	0.961	0.00053	0.278	0.142
ELM 4	1.477	0.245	0.959	0.00079	0.283	0.144
ELM 5	1.447	0.237	0.961	0.00106	0.277	0.141

Table 7 DR_{max}, DR_{min}, and DR_{ave} values for ELM models 1–5 and [11]

	Plume mass			Mass ratio			Y_{zero}		
	DR_{max}	DR_{min}	DR_{ave}	DR_{max}	DR_{min}	DR_{ave}	DR_{max}	DR_{min}	DR_{ave}
[11]	163,392.1	0.368	39.175	1,403,391	0.5618	342.861	109.803	0.545	1.250
ELM 1	2,108.627	0.0018	7.0281	483.6609	0.0037	2.765	104.356	0.032	1.073
ELM 2	4,098.162	0.003	6.490	1,045.368	0.0053	2.829	82.452	0.008	1.068
ELM 3	4,014.867	5.61E-05	6.495	335.291	0.0004	2.508	114.419	0.004	1.073
ELM 4	1,469.444	0.0005	6.133	537.4445	0.0017	2.575	63.755	0.003	1.062
ELM 5	2,311.012	0.006	6.335	822.4562	0.0010	2.652	65.876	0.022	1.060

systems in these areas would improve the quality of groundwater regarding reducing the salinity and would help treat more than 350 million m^3/year of wastewater produced from nearby treatment plants, I–V.

For the potential SAT sites in Egypt (as shown in Fig. 6), the average depth to groundwater is contained in Table 8 [36, 39, 40]. Table 8 presents the results of Sattar model study [11], and the model developed in this study for the zero concentration depth, i.e., the depth at which the concentration of OMPs reaches zero. The best locations for potential SAT system with the highest efficiency in removal of OMPs are Wadi El Natrun, Sadat City, and Alexandria, respectively, with an average removal efficiency of 90%. On the other hand, Rashed and Abu Rawash had the shallowest groundwater table disabling vadose soil to completely attenuate OMPs during wastewater infiltration, making these sites less favorable for SAT system construction. With the availability of detailed hydrogeological investigations for the potential SAT site, the uncertainty in model predictions [41–45], for OMP removal, can be significantly reduced, and the influence of SAT operational aspects can be studied.
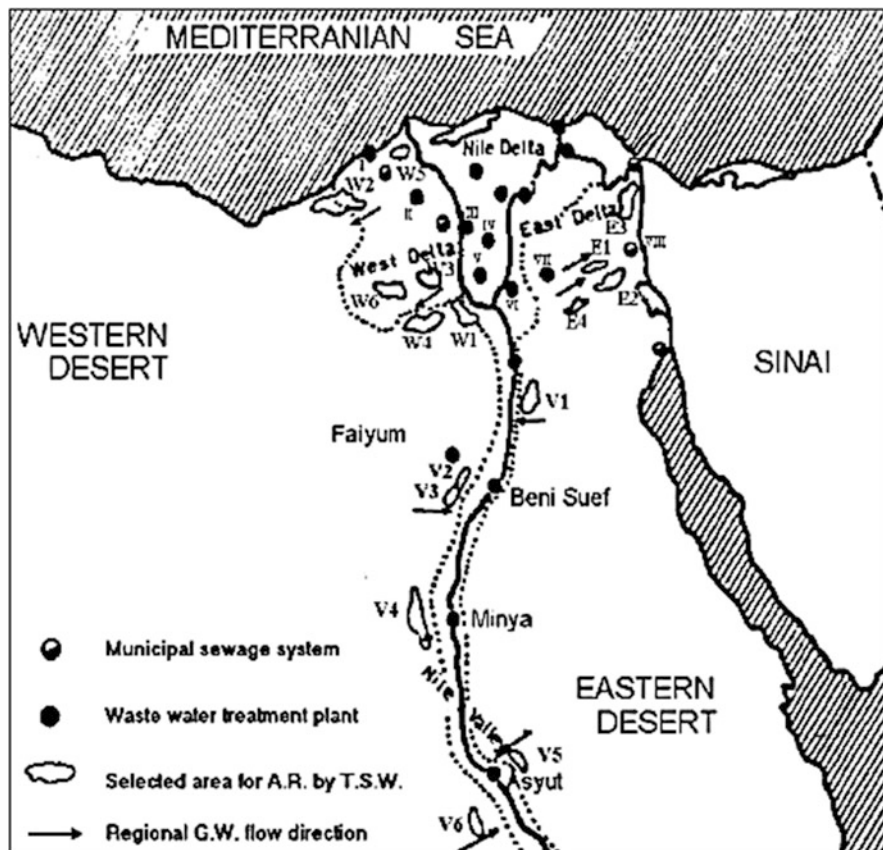
Fig. 6 Potential locations for construction of SAT systems in Egypt [38]

Table 8 Potential SAT system locations in Egyptian Western delta fringes and corresponding OMP removal

SAT location	Depth to groundwater table (m)	Removal of OMP (% from studied range)
Abu Rawash	4–7	20−60
Alexandria	3–14	10–90
Sadat City	15–25	95–100
Wadi EL Natrun	0–30	0–100
Rashed	1–5	5–50

7   Conclusions and Recommendations

One of the most important methods to remove organic micropollutants (OMPs) at water and wastewater treatment plants is using the soil aquifer treatment (SAT). In this study, the mechanism of organic micropollutant removal using extreme learning machine (ELM) method was evaluated. Therefore, five different ELMs for each

of the parameters' plume mass, mass ratio, and depth of concentration of 0% (Y_{zero}) were defined. Also, the results of extreme learning machine with results of gene expression programming model provided by [11] were compared. Analysis of numerical model results indicated the acceptable accuracy of ELM models in prediction of the pollutant removal efficiency during the SAT operation. Moreover, the model prediction accuracy of the optimum ELM model is assessed using the statistical performance parameters, including MARE, correlation coefficient, and scatter index, which were found to be 5.473, 0.970, and 0.746, respectively. Also, the discrepancy ratio for the parameter Y_{zero} by the best ELM model was calculated to be 1.060.

References

1. Sattar AM, Dickerson JR, Chaudhry MH (2009) Wavelet-Galerkin solution to the water hammer equations. J Hydraul Eng 135(4):283–295
2. Foda A, Sattar A (2013) Morphological changes in river Nile at Bani-Sweif for probable flood flow releases. In: Proceedings of the international conference on fluvial hydraulics, RIVER FLOW 2014, Switzerland
3. Sattar AM (2013) Using gene expression programming to determine the impact of minerals on erosion resistance of selected cohesive Egyptian soils. Experimental and computational solutions of hydraulic problems, part of the series geoplanet: earth and planetary sciences. Springer, Berlin, pp 375–387
4. Sattar AM (2014) Predicting morphological changes ds new Naga-Hammadi barrage for extreme Nile flood flows: a Monte Carlo analysis. J Adv Res 5(1):97–107
5. Sattar AM (2014) Gene expression models for prediction of dam breach parameters. J Hydroinf 16(3):550–571
6. Sattar AM (2014) Gene expression models for the prediction of longitudinal dispersion coefficients in transitional and turbulent pipe flow. J Pipeline Syst Eng Pract ASCE 5 (1):04013011
7. El-Hakeem M, Sattar AM (2015) An entrainment model for non-uniform sediment. Earth Surf Process Landf 4(9):1216–1226. https://doi.org/10.1002/esp.3715.
8. Sattar AM, Gharabaghi B (2015) Gene expression models for prediction of longitudinal dispersion coefficient in streams. J Hydrol 524:587–596
9. Najafzadeh M, Sattar AM (2015) Neuro-fuzzy GMDH approach to predict longitudinal dispersion in water networks. Water Resour Manag 29:2205–2219. https://doi.org/10.1007/s11269-015-0936-8
10. Sattar AM, Gharabaghi B, McBean E (2016) Prediction of timing of watermain failure using gene expression models. Water Resour Manag 30(5):1635–1651
11. Sattar AM (2016) Prediction of organic micropollutant removal in soil aquifer treatment system using GEP. J Hydrol Eng ASCE 21(9):04016027. https://doi.org/10.1061/(ASCE)HE.1943-5584.0001372
12. Sattar AM (2016) A probabilistic projection of the transient flow equations with random system parameters and internal boundary conditions. J Hydraul Res 54(3):342–359. https://doi.org/10.1080/00221686.2016.1140682
13. Sattar AM (2016) Closure to "gene expression models for the prediction of longitudinal dispersion coefficients in transitional and turbulent pipe flow" by Ahmed M. A. Sattar. J Pipeline Syst Eng Pract 7(4):07016002. https://doi.org/10.1061/(ASCE)PS.1949-1204.0000254

14. Thompson J, Sattar AM, Gharabaghi B, Richard W (2016) Event based total suspended sediment particle size distribution model. J Hydrol 536:236–246. https://doi.org/10.1016/j.jhydrol.2016.02.056
15. Sabouri F, Gharabaghi B, Sattar AM, Thompson AM (2016) Event-based stormwater management pond runoff temperature model. J Hydrol 540:306–316. https://doi.org/10.1016/j.jhydrol.2016.06.017
16. Atieh M, Taylor G, Sattar AM, Gharabaghi B (2017) Prediction of flow duration curves for ungauged basins. J Hydrol 545:383–394
17. Gharabaghi B, Sattar AM (2017) Empirical models for longitudinal dispersion coefficient in natural streams. J Hydrol. https://doi.org/10.1016/j.jhydrol.2017.01.022
18. Sattar AM, Gharabaghi B, Sabouri F, Thompson AM (2017) Urban stormwater thermal gene expression models for protection of sensitive receiving streams. Hydrol Process 31 (13):2330–2348. https://doi.org/10.1002/hyp.11170
19. El-Hakeem M, Sattar AM (2017) Explicit solution for the specific flow depths in partially filled pipes. J Pipeline Syst Eng Pract 8(4):06017004. https://doi.org/10.1061/(ASCE)PS.1949-1204.0000283
20. Sattar AM, Ertuğrul ÖF, Gharabaghi B, McBean EA (2017) Extreme learning machine model for water network management. Neural Comput Applic, 1–13. https://doi.org/10.1007/s00521-017-2987-7DO
21. Sattar AM, Beltagy M (2016) Stochastic solution to the water hammer equations using polynomial chaos expansion with random boundary and initial conditions. J Hydraul Eng 143(2):04016078. https://doi.org/10.1061/(ASCE)HY.1943-7900.0001227
22. Drillia P, Stamatelatou K, Lyberatos G (2005) Fate and mobility of pharmaceuticals in solid matrices. Chemosphere 60(8):1034–1044
23. Xu J, Wu L, Chang AC (2009) Degradation and adsorption of selected pharmaceuticals and personal care products (PPCPs) in agricultural soils. Chemosphere 77(10):1299–1305
24. Maeng SK, Sharma SK, Amy G (2011) Framework for assessment of organic micropollutant removals during managed aquifer recharge and recovery. Riverbank filtration for water security in desert countries. Springer, Dordrecht, pp 137–149
25. Yu Y, Liu Y, Wu L (2013) Sorption and degradation of pharmaceuticals and personal care products (PPCPs) in soils. Environ Sci Pollut Res 20(6):4261–4267
26. Lin C, Shacahr Y, Banin A (2004) Heavy metal retention and partitioning in a large-scale soil-aquifer treatment (SAT) system used for wastewater reclamation. Chemosphere 57 (9):1047–1058
27. Fox P, Aboshanp W, Alsamadi B (2005) Analysis of soils to demonstrate sustained organic carbon removal during soil aquifer treatment. J Environ Qual 34(1):156–163
28. Amy G, Drewes J (2007) Soil aquifer treatment (SAT) as a natural and sustainable wastewater reclamation/reuse technology: fate of wastewater effluent organic matter (EfOM) and trace organic compounds. Environ Monit Assess 129:19–26
29. Sharma SK, Harun CM, Amy G (2008) Framework for assessment of performance of soil aquifer treatment systems. Water Sci Technol 57:941–946
30. Caballero MH (2010) Soil aquifer treatment as pre-treatment for organic micropollutant removal during membrane filtration. MSc thesis, MWI 2019-5, UNESCO-IHE, Delft
31. Abel CDT, Sharma SK, Malolo YN, Maeng SK, Kennedy MD, Amy GL (2012) Attenuation of bulk organic matter, nutrients (N and P), and pathogen indicators during soil passage: effect of temperature and redox conditions in simulated soil aquifer treatment (SAT). Water Air Soil Pollut 223:5205–5220
32. Onesios-Barry KM, Berry D, Proescher JB, Sivakumar IA, Bouwer EJ (2014) Removal of pharmaceuticals and personal care products during water recycling: microbial community structure and effects of substrate concentration. Appl Environ Microbiol 80(8):2440–2450
33. Suzuki R, Kameda I, Takabe Y, Nishimura F, Itoh S (2015) Removal of dissolved organic matter and disinfection by-products formation potential in the upper layer during soil aquifer treatment. J Water Environ Technol 13(2):107–118

34. Huang GB, Zhu QY, Siew CK (2006) Extreme learning machine: theory and applications. Neurocomputing 70(1):489–501
35. Abokifa A (2013) Modeling soil aquifer treatment processes during managed aquifer recharge considering soil heterogeneity and parameter uncertainty. MSc thesis, Department of Irrigation and Hydraulics, Cairo University, Giza
36. Regional Institute for Groundwater Modeling (RIGW) (2006) Evaluation of different uses for the groundwater in Sadat city. Technical Report No. 3, Research Institute for Groundwater
37. El Arabi N, Mohamed A, Dawoud A (2012) Groundwater aquifer recharge with treated wastewater in Egypt: technical, environmental, economical and regulatory considerations. Desalin Water Treat 47:266–278
38. Fadlelmawal A, Halem M, Vissers M (1999) Preliminary plans for artificial recharge with reclaimed wastewater in Egypt. In: Proceedings, 9th biennial symposium on the artificial recharge of groundwater, Tempe
39. Abu Zeid K (2009) Assessment of groundwater potential in Alexandria governorate. Report submitted to sixth framework programme, CEDARE International
40. Ahmed MA, Abdel Samie SG, El-Maghrabi HM (2011) Recharge and contamination sources of shallow and deep groundwater of pleistocene aquifer in El-Sadat industrial city: isotope and hydrochemical approaches. Environ Earth Sci 62:751–768
41. Safadoust A, Amiri Khaboushan E, Mahboubi AA, Gharabaghi B, Mosaddeghi MR, Ahrens B, Hassanpour Y (2016) Comparison of three models describing bromide transport as affected by different soil structure types. Arch Agron Soil Sci 62(5):674–687. https://doi.org/10.1080/03650340.2015.1074184
42. Gharabaghi B, Safadoust A, Mahboubi AA, Mosaddeghi MR, Unc A, Ahrens B, Sayyad G (2015) Temperature effect on the transport of bromide and E. coli NAR in saturated soils. J Hydrol 522:418–427. https://doi.org/10.1016/j.jhydrol.2015.01.003
43. Safadoost A, Yousefi G, Mahboubi A, Gharabaghi B, Mosaddeghi M, Yousefi G, Safadoust A, Mahboubi AA, Gharabaghi B, Mosaddeghi MR, Ahrens B, Shirani H (2014) Bromide and lithium transport in soils under long-term cultivation of alfalfa and wheat. Agric Ecosyst Environ 188:221–228. https://doi.org/10.1016/j.agee.2014.02.031
44. Safadoust A, Mahboubi AA, Mossaddeghi MR, Gharabaghi B, Unce A, Voroney P, Heydari A (2012) Effect of regenerated soil structure on unsaturated transport of Escherichia coli and bromide. J Hydrol 430–431:80–90. https://doi.org/10.1016/j.jhydrol.2012.02.003
45. Safadoust A, Mahboubi AA, Gharabaghi B, Mosaddeghic MR, Voroney P, Unce A, Khodakaramian G (2012) Significance of physical weathering of two-texturally different soils for the saturated transport of E. coli and bromide. J Environ Manag 107:147–158. https://doi.org/10.1016/j.jenvman.2012.04.007